

# Appendix A

## Measurement and Application of Ground Tilt and Classification of Earthquakes and Earthquake Swarms at Kilauea

*Discusses the establishment of the long-term viability of daily tilt measured in the Whitney Vault, provides definitions of the seismic regions of Kilauea Volcano and of earthquake swarms, and presents our methodology for calculating magma supply rates.*

Webcams on the edge of the Kilauea Caldera, monitored by HVO.



## Tilting of the Ground

Tilt in volcanology is the change in slope of the ground measured between two instants in time. It is important to specify the beginning and ending times of measurement to evaluate a tilt change, and in a time series tilt is measured relative to the initial value of the slope. Tilt is an angle measured in microradians<sup>1</sup> or seconds of arc. Tilting of the ground at Kīlauea's summit is one method by which one can infer the amount of inflation or deflation of the volcano and locate the depth of the magma reservoir from which eruptions are fed. Tilt is the only frequent measure of ground deformation that extends from the present back in time to the founding of the Hawaiian Volcano Observatory (HVO) in 1912.

## Tilt Measurement

Tilt is a vector measured as two perpendicular components, north-south ( $u$ ) and east-west ( $v$ ), measured from an arbitrary starting point ( $u_0, v_0$ ). Tilt values are expressed as a vector with a magnitude and an azimuth. Tilt magnitudes extending back in time to an arbitrary starting point are calculated as  $[(u-u_0)^2+(v-v_0)^2]^{1/2}$ . Tilt magnitudes depend on the choice of origin ( $u_0, v_0$ ), but changes in tilt magnitude are relatively free of origin choice if (1) the origin is far from the current tilt value, (2) the tilt change is much smaller than the total size of the tilt magnitude, and (3) the azimuth does not change much during the measurement interval. Tilt magnitudes for daily measurements made in the two vaults at Kīlauea are shown on the time-series plots in this report as calculated from arbitrary values assigned at the time of

installation of the tiltmeter. Such plots show the cycles of inflation and deflation of Kīlauea's summit over the lifetime of the tiltmeter. The tilt azimuth formulas are constructed such that pairs of north-south and east-west vectors, respectively,  $[1, 1]$ ,  $[-1, 1]$ ,  $[-1, -1]$ ,  $[1, -1]$  yield azimuths of 45, 135, 225, and 315 degrees. Tilt vectors are conventionally plotted as arrows pointing in the downward (deflation) direction at the calculated azimuth.

## Nature of the HVO Tilt Networks

The original site for tilt measurement was the Whitney Vault, located adjacent to the present-day Volcano House Hotel on the northeast rim of Kīlauea Caldera. Tilt was measured daily using a Bosch-Omori seismometer, and components of the tilt vector were recorded in the Weekly and Monthly Bulletins of the Hawaiian Volcano Observatory (HVO) (Bevens and others, 1988) and later in The Volcano Letter (Fiske and others, 1987) to give a continuous time history (see figs. in chaps. 2–4). A vault built in 1948 a few hundred meters back of Uwēkahuna bluff near the Volcano Observatory was refurbished in 1957. Jerry Eaton installed a water-tube tiltmeter of his design (Eaton, 1959) in both the Uwēkahuna and Whitney Vaults (fig. A2 and appendix I), and these instruments were also read daily in parallel from 1957 until the abandonment of the Whitney Vault at the end of 1962 (fig. A1). The three datasets were never published, but they were obtained from the HVO data archives. Plotted together with simple linear scaling, the three datasets show remarkable agreement (fig. A1). This gives us confidence to use the long-term (1912–62) Whitney seismic tilt as a reliable indicator of ground movements at Kīlauea's summit. Using both tiltmeters, we choose the 1960–61 and

1966–67 time periods for our example calculations (appendix I). The 1960–61 cycle adds credence to the use of Whitney tilt back in time as a surrogate for volume of summit magma accumulation. During the period between 1961 and 1967, tilt and level surveys were measured frequently and several large inflation-deflation cycles were captured.

Eaton also installed a field network of arrays of concrete piers, arranged in triangles approximately 50 meters on a side (Eaton, 1959), on which water-tube tiltmeters could be placed and read. This network was occupied periodically, at intervals of several months and always after a major event such as an eruption, intrusion, or very large earthquake. Station locations are also shown in appendix I. The water-tube tilt network had two limitations common to any periodic surveys to measure vertical and horizontal movements of the ground; these are that (1) one could always measure the state of the ground following an event, but one had to be very lucky to occupy a network just preceding such an event, and (2) the surveys took several days to complete, during which the ground was moving, and not necessarily in the same way at each station.

## Source of Tilt Changes

At the time of the founding of the Hawaiian Volcano Observatory (HVO) there were only sketchy ideas about the source of magma for Kīlauea's eruptions. The Japanese seismologist Kiyoo Mogi modeled leveling and triangulation surveys made both before and after the large collapse at Kīlauea's summit in 1924 (Mogi, 1958). From this study and his study of Japanese volcanoes he concluded that ground deformation measured at various volcanoes could be modeled as responding to a spherical or point source of magma located several kilometers

---

<sup>1</sup>1 microradian ( $\mu$ r) = 0.2063 sec; 1 sec = 4.8468  $\mu$ r

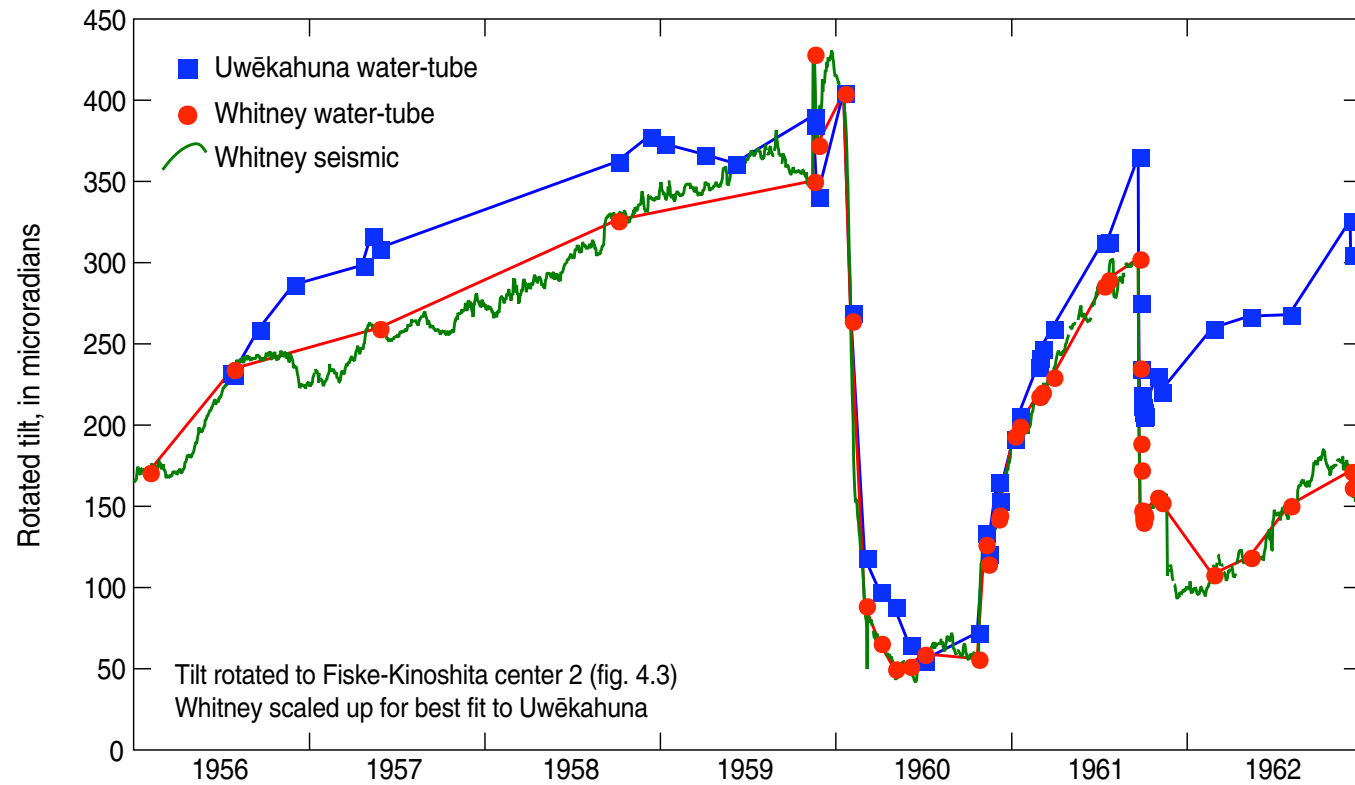


**Figure A1.** Graph comparing three tilt records at Kilauea for the overlap time after the installation of the Uwēkahuna Vault in 1956 and before the abandonment of the Whitney Vault in 1963. Comparison is of measurements made by short-base water tube tiltmeters installed in Uwēkahuna (blue points) and Whitney (red points) Vaults with the tilt measured by the Bosch-Omori seismometer installed in The Whitney Vault (green line). The time of overlap is between mid-1956 and the end of 1962. Tilt data are rotated to Fiske-Kinoshita center 2 (fig. A2), and the Whitney water-tube data are scaled to fit the Uwēkahuna water-tube data. The excellent agreement indicates that the tiltmeters track each other and provide a firm basis for interpreting the Whitney seismic tilt, the only available tilt measurement between 1912 and 1956. The time period covered includes the major eruptions and deflations in January 1960 and September 1961. The approximate coincidence of the three tilt functions demonstrates they all measure the same inflation/deflation bulge. The divergence of Uwēkahuna and Whitney tilt after August 1961 means the deflation and inflation location shifted relative to the inflation in the 1950s and the 1960 collapse and recovery. The tilt scale on the figure refers to the Uwēkahuna water tube tilt. The Uwēkahuna tilt vector  $\tau$  is measured frequently, and we seek tilt rotated to the azimuth  $-67$  degrees pointing from the Fiske-Kinoshita (1969) deflation center 2. The plotted Uwēkahuna water tube tilt function is  $T_U = [\cos(-67^\circ) \tau_N + \sin(-67^\circ) \tau_E] + 500$ . The offset of 500 microradians is the arbitrary baseline chosen when measurements started and is not determined by any data fitting. The Whitney seismic tilt vector  $\tau$  was measured daily as the offset of the pendulum of the north and east components of the Bosch-Omori seismometer, and we seek the component rotated to the azimuth  $45$  degrees pointing from the deflation center 2 in figure A2. The plotted Whitney seismic tilt function is  $T_{WS} = 8.2 [\cos(45^\circ) \tau_N + \sin(45^\circ) \tau_E] - 150$ . The linear scaling factor (8.2) and the offset ( $-150$ ) are determined empirically to fit the tilt functions from the two vaults. The Whitney water tube tilt vector  $\tau$  was measured frequently, and we plot the tilt rotated to the azimuth  $45$  degrees pointing from the inflation center 2 in figure A2. The plotted Whitney water tube tilt function is  $T_{WW} = 8.2 [\cos(45^\circ) \tau_N + \sin(45^\circ) \tau_E] - 165$ . The scaling factor (8.2) was determined by the seismometer tilt fit, and the offset ( $-165$ ) adjusts for the arbitrary baseline.

beneath the volcano's summit. Jerry Eaton expanded on Mogi's work to clearly recognize the existence of an approximately spherical magma reservoir located about 4 km beneath Kīlauea's summit (Eaton, 1962). Addition of magma to this reservoir caused the ground above to expand upward and outward (inflation), and the reverse happened (deflation) when magma left the reservoir to feed eruptions and intrusions. Thus the tiltmeters located around Kīlauea's summit faithfully recorded cycles of inflation and deflation.

As a context for interpreting the time-history of tilt changes at Kīlauea's summit we rely on the careful leveling surveys made in the period preceding the 1967–68 eruption in Halema'uma'u (Fiske and Kinoshita, 1969, fig. 5). They documented an apparent migration of centers of inflation from north to south and then to the west, with some movement back and forth. The locations of these centers, and the two vaults where tilt was measured daily, are shown in figure A2. Mogi and Eaton's idea of a single point source was modified to identify multiple centers of inflation and deflation within a broader, and only approximately spherical, source region covering a depth range of 2–6 km beneath Kīlauea's summit. Most modeled centers occur between 2 and 4 km depth. The consequences of this source complexity is that tilt vectors from the summit network almost never intersect at a point because each station responds more to the nearest source(s) and less to the more distant sources. One additional complexity is the existence of deformation at several places along the east rift zone, documented in several published studies (see, for example, Wright and Klein, 2006, fig. 2 and references cited therein). The Whitney Vault appears to respond to deformation within the east rift zone as well as to summit inflation/deflation cycles, because the azimuths of Whitney tilt often point to the east of the Fiske-Kinoshita centers.

In this report we are mainly concerned

with tilt changes during the short periods of time associated with intrusions, eruptions, and earthquake swarms. These values are independent of any assumptions regarding starting values and, subject to the assumption of similar sources, allow accurate comparison of tilt changes for events occurring at different times in Kīlauea's history. Complete formulations of the tilt equations, including the conversion from tilt magnitude to magma volume, are given in appendix I. During the days associated with a volcanic event, tilt vectors may change direction during deflation and reinflation to indicate draining and filling of different parts of the reservoir complex as represented by the Fiske-Kinoshita centers shown in figure A2. Many events show a hysteresis involved in deflation and reinflation, in which deflation vectors may migrate clockwise (from the Uwēkahuna Vault), indicating draining of the northernmost parts of the magmatic system first, and reinflation also occurs first to the north. However, extended periods of deflation or inflation may show vectors that point outside of the range of Fiske-Kinoshita centers. For example, in the early stages of deflation the north-south and east-west tilt components change together. Later the north-south or east-west component may continue in the same direction while the other component remains unchanging or may begin to reverse direction. By simple vector addition one can interpret this behavior as the beginning of resupply to one source while another source continues to drain.

## Whitney Tilt Volume Calculations

In an effort to determine magma center volume changes from a single tiltmeter, we examine the simpler period of 20 January to 1 April 1960, during which Kīlauea's summit underwent a massive deflation associated with the east rift eruption of 13

January to 19 February 1960. Unfortunately there is no level survey for this interval, but the deflation is included in a longer interval from January 1958 to May 1960 for which a level survey exists (appendix I, table I1, event 1). We can use this 1960 deflation as an example of estimating source depth from two tiltmeters and volume change from a single tiltmeter. The tilts are 275 and 199 microradians, and the source distances are 3.2 and 3.8 km for the short-base water tubes at Uwēkahuna and Whitney, respectively (fig. A3). Equation 6 in appendix I thus yields a source depth of 3.0 km. Comparison of measured tilts and a Mogi source at 3.0 km depth (appendix I) confirm the 3.0-km depth and a volume of  $0.107 \text{ km}^3$  as a good fit to the tilt data, excluding Ke'āmoku as an amplified site. The tradeoff between volume and source depth of the three curves of appendix I, figure I4, means that for variation of  $\pm 0.5 \text{ km}$  from its average source depth of 3.0 km, the magma volumes vary by  $\pm 20$  percent (table A1). Thus either tiltmeter, when used alone, gives usable volume estimates. The factor of 0.00045 used by Dvorak and Dzurisin (1993) corresponds to a depth between 3 and 3.4 km at the centers in the south caldera most frequently seen in tilt vectors for inflation and deflation (table A1). From table A1 the ratio of Whitney to Uwēkahuna tilt for a depth of 3 km is 1.38. We apply this ratio to the Dvorak factor for Uwēkahuna of  $0.00045 \text{ km}^3/\text{microradian}$  to yield  $0.000621 \text{ km}^3/\text{microradian}$  for the conversion of Whitney tilt magnitude to volume. We use this factor for the volume calculations during periods before 1960 when the only tilt magnitudes were calculated in seconds of arc at the Whitney Vault.

The theoretical volume factor for the Whitney tiltmeter and the 1960 deflation source is  $D_{WT}=0.00049 \text{ km}^3/\text{microradian}$ , which is somewhat larger than the Uwēkahuna factor because Whitney is farther from the source. The empirical factor for Whitney is  $D_{WE}=0.00054$

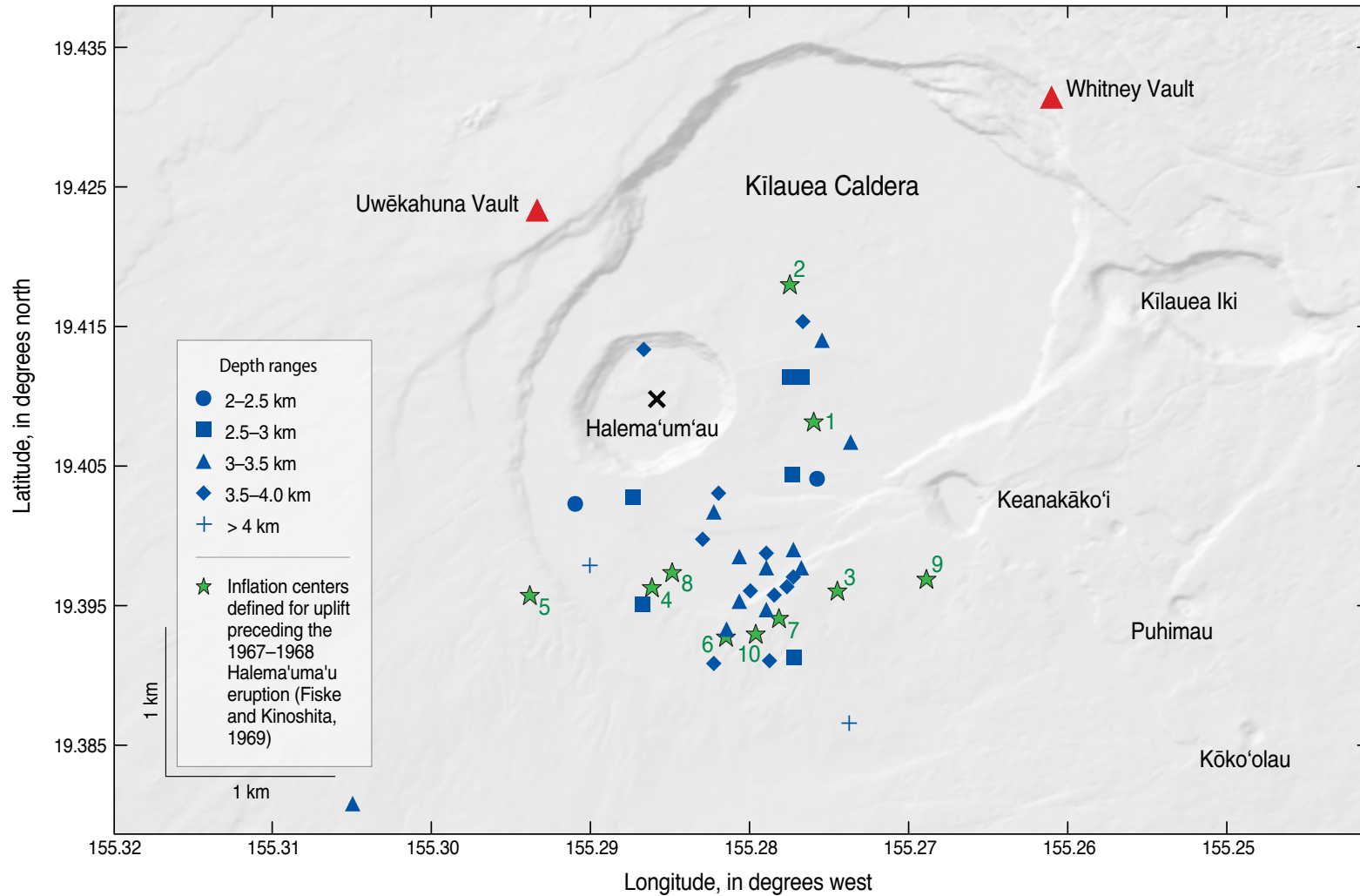


**Figure A2.** Map showing locations of inflation-deflation centers at Kilauea. Tiltmeter locations are shown as red triangles. The green stars are centers of inflation from leveling surveys conducted during the inflation preceding the 1967–68 Halema'uma'u eruption (Fiske and Kinoshita, 1969, figure 5). The blue symbols (keyed to depth) are inflation and deflation centers determined in this study and listed in appendix I table I1.

**Table A1.** Volume factors ( $\text{km}^3/\mu\text{rad}$ ) for continuous tiltmeters for various summit Mogi sources at Kilauea<sup>1</sup>.

Caldera centers	South centers <sup>2</sup>	South centers 6, 7, 10 <sup>3</sup>	Central center 1	SE center 9	NE center 2
A. Uwēkahuna					
Distance (km)	3.2	3.5	2.7	4	1.77
Depth (km)					
2.5	0.000317	0.000386	0.000229	0.000536	0.000140
3	0.000388	0.000455	0.000303	0.000597	0.000222
3.5	0.000491	0.000556	0.000410	0.000695	0.000344
4	0.000632	0.000695	0.000556	0.000831	0.000519
B. Whitney					
Distance (km)	3.8	4.2	2.9	3.5	2.16
Depth (km)					
2.5	0.000471	0.000611	0.000261	0.000387	0.000168
3	0.000536	0.000668	0.000334	0.000456	0.000245
3.5	0.000636	0.000764	0.000439	0.000557	0.000358
4	0.000773	0.000898	0.000583	0.000696	0.000516

<sup>1</sup>Values include a +10-percent empirical correction. See text.

<sup>2</sup>Calculated for the average location of unnumbered centers of inflation and deflation plotted in figure A2.

<sup>3</sup>Numbered centers shown in figures A2 and A3

$\text{km}^3/\text{microradian}$ . The theoretical volume factors for Whitney also require a 10-percent correction. Using equation 5 and typical deformation centers (appendix I; table A1), we can calculate a table of tiltmeter volume factors for various Mogi locations and depths and apply the 10-percent empirical correction (see table A1). The Dvorak factor for Uwēkahuna that we use ( $0.00045 \text{ km}^3/\text{microradian}$ ) yields a depth of  $\sim 3.8 \text{ km}$  for the central caldera source in table A1.

## Uncertainty of Whitney Tilt Magnitudes

Whitney tilt data were considered in the early literature to be affected by seasonal variations to explain the apparent tilt cycles in the tilt record between 1925 and 1950. It is easy to dismiss the lack of precise correlation of the Whitney tilt with events at Halema‘uma‘u as due to errors in the use of a recently installed instrument, and one primarily designed to measure earthquakes. Indeed, the instrument used as a tiltmeter was said to be affected by factors related to both diurnal and seasonal changes (Jaggar and

**Table A2.** Whitney tilt rainfall correlation and magnitude error.

[Dates in m/dd/yyyy format]

Dates	Az.	M ( $\mu\text{rad}$ )	std <sup>1</sup>	$\Delta t^2$	in/day <sup>3</sup>	std <sup>4</sup>	Comment
9/13/1925–2/13/1926	207	0.65	5.41	153	0.14	0.27	Flat tilt
7/9/1932–9/6/1932	259	2.97	3.59	59	0.09	0.11	do <sup>5</sup>
5/8/1938–9/2/1938	255	3.32	3.77	117	0.17	0.18	do
11/17/1929–1/16/1930	192	14.18		60	0.41	1.01	Sharp deflation
2/2/1932–3/25/1932	184	42.86		52	0.39	0.53	do
12/25/1936–2/21/1937	188	66.97		58	0.86	1.30	do
8/19/1920–12/7/1920	349	1.48	3.13	111	0.21	0.34	No volcanic event
8/25/1921–10/20/1921	84	2.92	2.58	56	0.24	0.38	No volcanic event

<sup>1</sup>Standard deviation of magnitude for the time intervals of little tilt change. Not calculated for periods of large tilt change

<sup>2</sup>Time interval in days.

<sup>3</sup>The standard deviation is calculated for the days within the period for which rainfall was recorded.

<sup>4</sup>Standard deviation in inches of rain per day.

<sup>5</sup>Do, ditto (same as above).

Finch, 1928; Powers, 1946; Powers, 1947). In fact, no seasonal changes could be verified (Powers, 1947). We tested the effects of heavy rain and calculated the standard deviation of tilt changes in periods of little expected volcanic tilt change (table A2). For three large apparent deflations in the 1925–39 period uncorrelated with volcanic events we show a strong correlation with high average rainfall (table A2). Periods of little tilt change are correlated with low average rainfall (table A2). We suspect that much of the cyclic change in the 1925–50 period is due to high rainfall and to recovery from it.



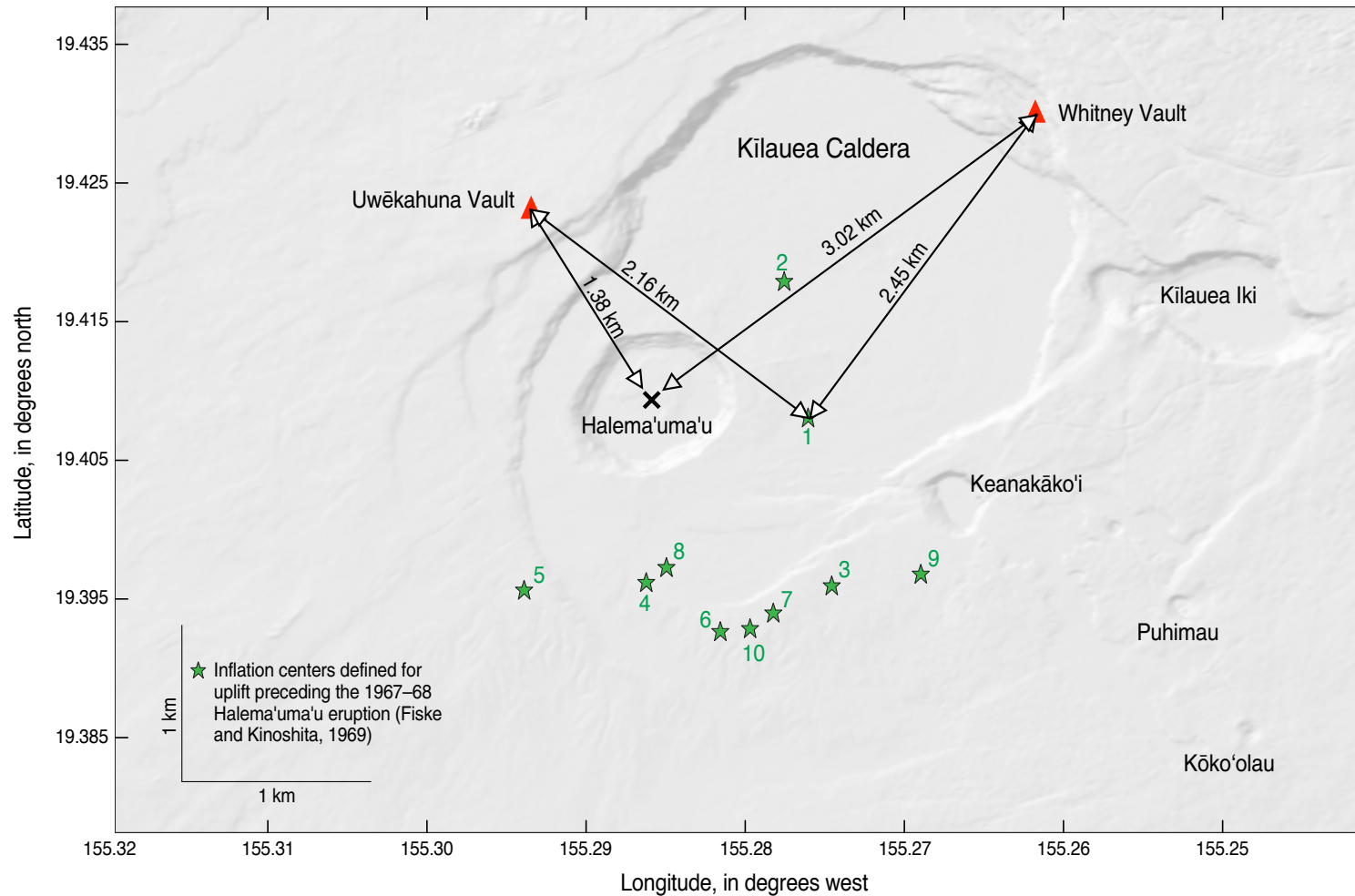


**Figure A3.** Map comparing geographic relations of the Whitney and Uwēkahuna Vaults. The Whitney Vault is at a much greater horizontal distance from Halema'uma'u, so that removal of magma from a shallow (<1 km) source, including the rise and fall of lava in Halema'uma'u lava lake is not measured at the Whitney Vault, whereas such events are easily detected at Uwēkahuna. The slant distances to the shallow reservoir at 2–6 km depth are more nearly comparable, such that both vaults record magma addition and removal from that reservoir, including addition of magma below inflation centers identified during the buildup to the 1967–68 Halema'uma'u eruption (Fiske and Kinoshita, 1969). These centers are also the locus of inflation/deflation for both earlier and later intrusions and eruptions. The Whitney Vault is close to Kilauea Iki Crater and closer to the upper east rift zone compared to the Uwēkahuna Vault and therefore can record changes associated with shallow magma storage at both locations that could not be noticed at Uwēkahuna.

**Table A3.** Presentation and interpretation of seismicity.**A. Earthquake Classification by Tectonic Region.**

Code	Depth (km) <sup>1</sup>	Location (see text figure 1.3)
ms1	0–5	Magma supply path beneath Kīlauea’s summit, including some earthquakes north of Kīlauea Caldera
ms2	5–10	Magma supply path beneath Kīlauea’s summit, including some earthquakes north of Kīlauea Caldera
ms3	10–20	Magma supply path beneath Kīlauea’s summit, including some earthquakes north of Kīlauea Caldera
ms4	20–35	Magma supply path from the Hawaiian hotspot to beneath Kīlauea’s summit
ms5	>35	Magma supply path from the Hawaiian hotspot to beneath Kīlauea’s summit
ms5gln	>35	Unique earthquake swarms north of Kīlauea Caldera and east rift zone
ei1ler	0–15	Lower east rift zone—continuation of east rift zone east from Heiheiāhulu; continues offshore for 50 km
ei2mer	0–15	Middle east rift zone—east-trending east rift zone defined by surface fractures, shields and cinder cones and pit craters; active vents extend from Mauna Ulu to Heiheiāhulu
ei3uer	0–15	Upper east rift zone—southeast-trending rift zone defined by surface fractures, cones and pit craters. Turns east at intersection with Koa’e fault system; active vents extend from Puhimau to Mauna Ulu
ei4sswr	0–15	Seismic southwest rift zone—locus of earthquake swarms trending south from Halema’uma’u, then southwest to join southwest rift zone in the vicinity of the Kamakai’a Hills; locus of intrusions
ei5swr	0–15	Southwest rift zone—defined by surface fractures, cones and pit craters; locus of eruptions and intrusions
koa	0–15	Koa’e Fault Zone—the region between the southwest and east rift zones; bounded on the north by the northernmost set of active east-west fractures; bounded on the south by the Kalanaokuaiki north-facing fault scarp
sf1ler	0–15	Far eastern south flank—south of lower east rift zone
sf2mer	0–15	Eastern south flank—south of middle east rift zone; site of large-magnitude south flank earthquakes
sf3kuer	0–15	Central south flank—south of Koa’e Fault Zone and west of upper east rift zone
sf4swr	0–15	Western south flank—east of southwest rift zone and southwest of Koa’e Fault Zone

<sup>1</sup>Depths are coded on time-series plots. Earthquakes at depths less than 20 km are mostly within the Kīlauea edifice above the decollement. Most events are shallower than 12 km. The few events whose depths are between 15 and 20 km may be mislocated. Earthquakes deeper than 20 km beneath the middle and lower east rift zones and eastern and far eastern south flank fall off the magma supply path and are related to other mantle processes, including response to Pacific Plate motion. These infrequent events are plotted but not interpreted in this report.

**B. Definition of Earthquake Swarms****Earthquake swarms****1. Periods of eruption and (or) shallow intrusion in regions ms1, ei1-5 and koae.** Depth range 0–5 km.

Earthquake swarms comprise a contiguous period during which events in a region occur at a frequency of greater than 1 event every 6 hours.

Earthquake swarms commonly consist of at least 10 events.

**2. Elevated subcaldera activity in regions ms2 and ms3 or rift activity in regions ei2-5.** Depth range 5–20 km.

Earthquake swarms comprise a contiguous period during which events in a region occur at a frequency of greater than 1 event every 6 hours.

Earthquake swarms commonly consist of at least 5 events.

**3. Elevated deep activity along magma supply path in regions ms4-5, koae, ei3-5, and sf 2-4.** Depth range >20 km.

Earthquake swarms comprise a contiguous period during which events in a region occur at a frequency of greater than 1 event every 6 hours.

Earthquake swarms commonly consist of at least 5 events.

**4. Elevated south flank activity.** Depth range 0–15 km.

Earthquake swarms comprise a contiguous period during which events in a region occur at a frequency of greater than 1 event every 6 hours.

Earthquake swarms commonly consist of at least 5 events.



We also calculated the standard deviation of calculated magnitude for periods of low tilt change (table A2, column 4) and found two standard deviations to be less than 10 microradians, in agreement with an uncertainty estimate made during transcription of written records to a computer file (A. Okamura, oral commun., 2011).

## Earthquake Swarms

Earthquakes are assigned to regions of the volcano, which are named and described in table A3A and shown in map view on figure A4. Earthquake swarms precede nearly all eruptions and are critical to the identification of intrusions. Earthquake swarms in all regions are defined as a sequence of at least 5–10 earthquakes within a single region (fig. A4) with a time difference from one to the next of less than 6 hours. Additional description of plotting parameters is given in table A3B.

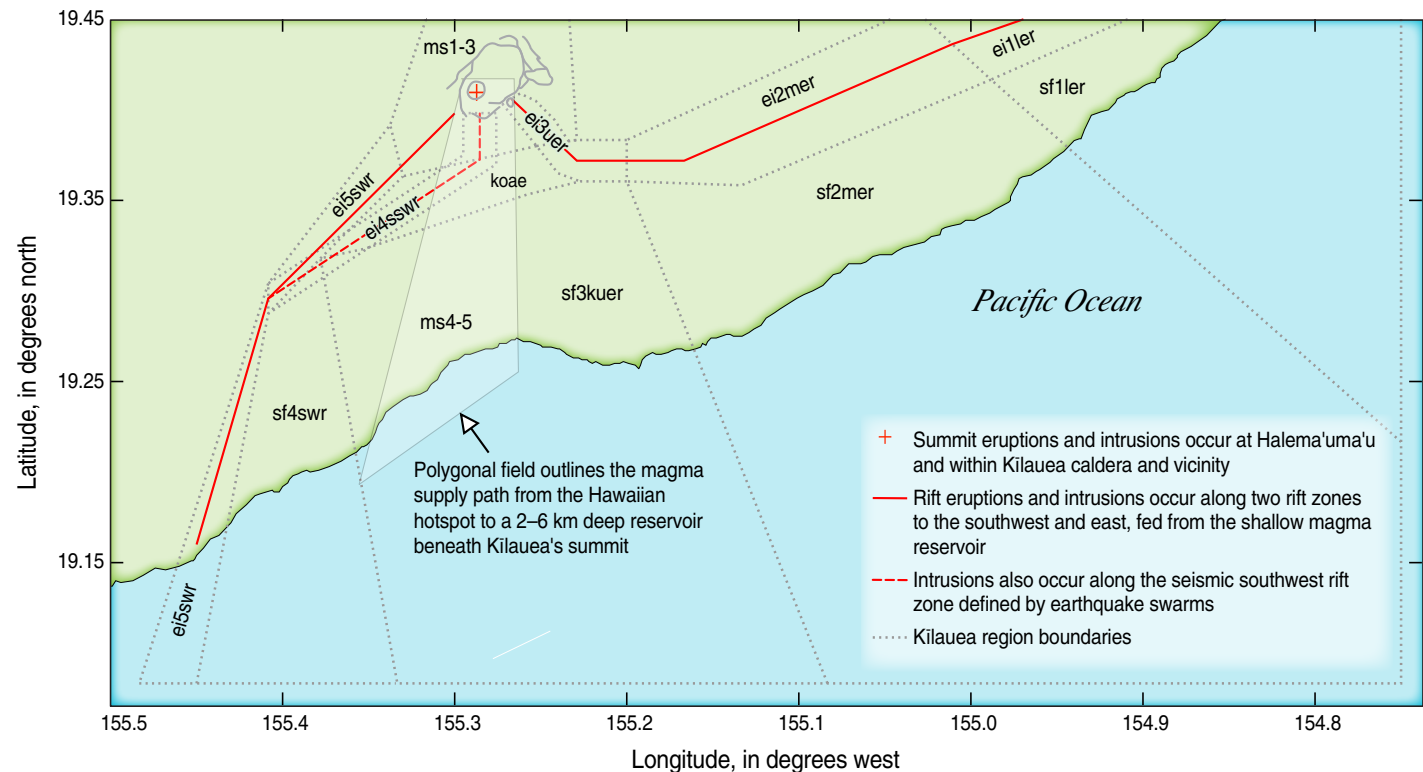


**Figure A4.** Map showing regional classification of earthquakes and naming of regions of Kilauea. Seismic regions are labeled according to tectonic regions described in table A3. The region abbreviations are used in numerous figures in this report: “ms” stands for m(agma) s(upply), and numbers from 1 to 5 correspond to different depth ranges along the magma supply path from the mantle defined by Wright and Klein (2006). Magma supply regions 1–3 lie below Kilauea’s summit at depths shallower than 15 km. Magma supply regions 4 (20–35 km) and 5 (>35 km) extend from north of Kilauea’s summit south and southwest beneath the Koa’e Fault Zone and both onshore and offshore parts of Kilauea’s central and western south flank. The magma supply path boundary is shown in the background of all plots that show earthquake locations. “ei” stands for e(ruption) i(ntrusion), and regions 1–5 correspond to earthquakes beneath the rift zones extending in a counterclockwise direction from the easternmost “lower east rift” through the westernmost “southwest rift.” “koa’e” separately designates the Koa’e Fault Zone, which connects the two rift zones. “sf” stands for s(outh)f(lank), and south flank regions 1–4 extend counterclockwise adjacent to the rift segments and the Koa’e Fault Zone. Rift, south flank, and Koa’e earthquakes occur at depths shallower than 15 km, and, allowing for some depth error, their hypocenters lie above the decollement at 10–12 km.

## Calculation of Magma Supply and Eruption Efficiency

A principal focus of this study is to calculate both spreading rates and magma supply rates over time. Magma supply and spreading rates in the modern era have been summarized elsewhere (Wright and Klein, 2008) and are reevaluated in this report. We rely on rates at which magma is added to the surface to represent a minimum supply rate. Volumes of vesiculated lava are reduced by 20 percent to yield an equivalent magma volume before calculating the rate as km<sup>3</sup>/yr.

### 19th Century: Calculation of Magma Supply from Caldera Filling Rates

For events in the 19th century we estimate magma supply rate from the volumes of filling and draining of Kīlauea Caldera, to which are added a hypothesized estimate of deep endogenous growth related to rift dilation during intrusion. Magma filling is a gradual process, for which rate calculation is possible, but drainings are generally sudden events, and only a volume estimate can be made. Just like the tilt record and inferred inflation level measured in later years of observation by HVO, the level of a lava lake is a proxy for the inflation state and can be visualized as a gradual up and sudden down sawtooth function. We calculate draining volumes (chapter 2, table 2.2) as combinations of cylinder, cone frustum, or half an oblate spheroid, depending on the description given in the literature cited. Filling (chapter 2, table 2.5) is calculated using the same formulations, but with lava volumes converted to magma equivalents as above. Filling rates are calculated for intervals bounded by more definitive data on lava added to the caldera and (or) prior to

major drainings. The volume calculated includes the amount of magma needed to fill any draining volumes before the end of the period added to the volume of new magma equivalents added to the caldera floor.

### 1894–1950: Calculation of Magma Supply from Filling of Halema‘ūma‘u Crater and Tilt

In this period we apply the same methodology as above for filling and draining of Halema‘ūma‘u and factor in volume changes from deflations accompanying the 1922 east rift eruption and the 1924 draining of Halema‘ūma‘u.

### Post-1950: Calculation of Magma Supply from Tilt

From the beginning of reinflation of Kīlauea in 1950, it is possible to consider volumes of inflation and deflation to augment eruption rates in calculating magma supply. Spreading rates are crudely estimated for times preceding the installation of a continuously recording geodetic network. We use summit tilt magnitude as a surrogate for magma volume moving in or out of the summit reservoir. Summit inflation is equated to magma addition to the summit reservoir. Summit deflation is equated to magma transfer to the rift zone(s). We assume that, because of buoyancy, magma never retreats down the vertical supply path, which could be an alternate interpretation for summit deflation. We calculate volumes using the same tilt-to-volume factor as previously published (Dvorak and Dzurisin, 1993). At times when the Whitney Vault houses the only tiltmeter we increase the volume factor by about 1.6, based on comparison of Uwēkahuna and Whitney tilt during the period of overlap (fig.

A1). Our calculations ignore the possibility of magma compression during storage or decompression during transfer to the rift zone (Johnson, 1992; Johnson and others, 2000; Rivalta and Segall, 2008)<sup>2</sup>. Our estimates of volume thus may be slightly underestimated for summit inflation and slightly overestimated for summit deflation. We treat tilt data differently in the magma supply calculations for periods of (1) noneruption, (2) summit and continuous rift eruptions, and (3) short rift eruptions accompanied by summit deflation. During noneruptive times an increase of tilt magnitude when the azimuth indicates inflation is interpreted as addition of magma to Kīlauea’s summit reservoir and is treated as a positive magma volume quantity. A short period of deflation reflects transfer of magma to the rift zones and is also treated as a positive quantity, but magma counting is based on the deflation volume and the succeeding period of recovery is not independently counted. During eruption at Kīlauea’s summit, an inflation azimuth reflects addition of magma to Kīlauea’s shallow reservoir, whereas a deflation azimuth reflects transfer of magma to the rift zones. The tilt magnitudes associated with both are counted as positive quantities in the magma supply calculations, and the rate of magma supplied from depth over the period of eruption always exceeds the rate of eruption. At the beginning of summit eruptions the initial eruption rate may temporarily exceed the supply rate, resulting in a small deflation reflecting a temporary drawdown of the summit reservoir. Rapid inflation of the summit during summit eruptions

---

<sup>2</sup>The effects of compression occur only at the end stages of long inflations, thus have little effect on the overall tilt change. Decompression occurs virtually immediately at the onset of deflation preceding and accompanying magma transfer to the rift zone. Thus the overall tilt change associated with deflation is likewise barely affected by the decompression.

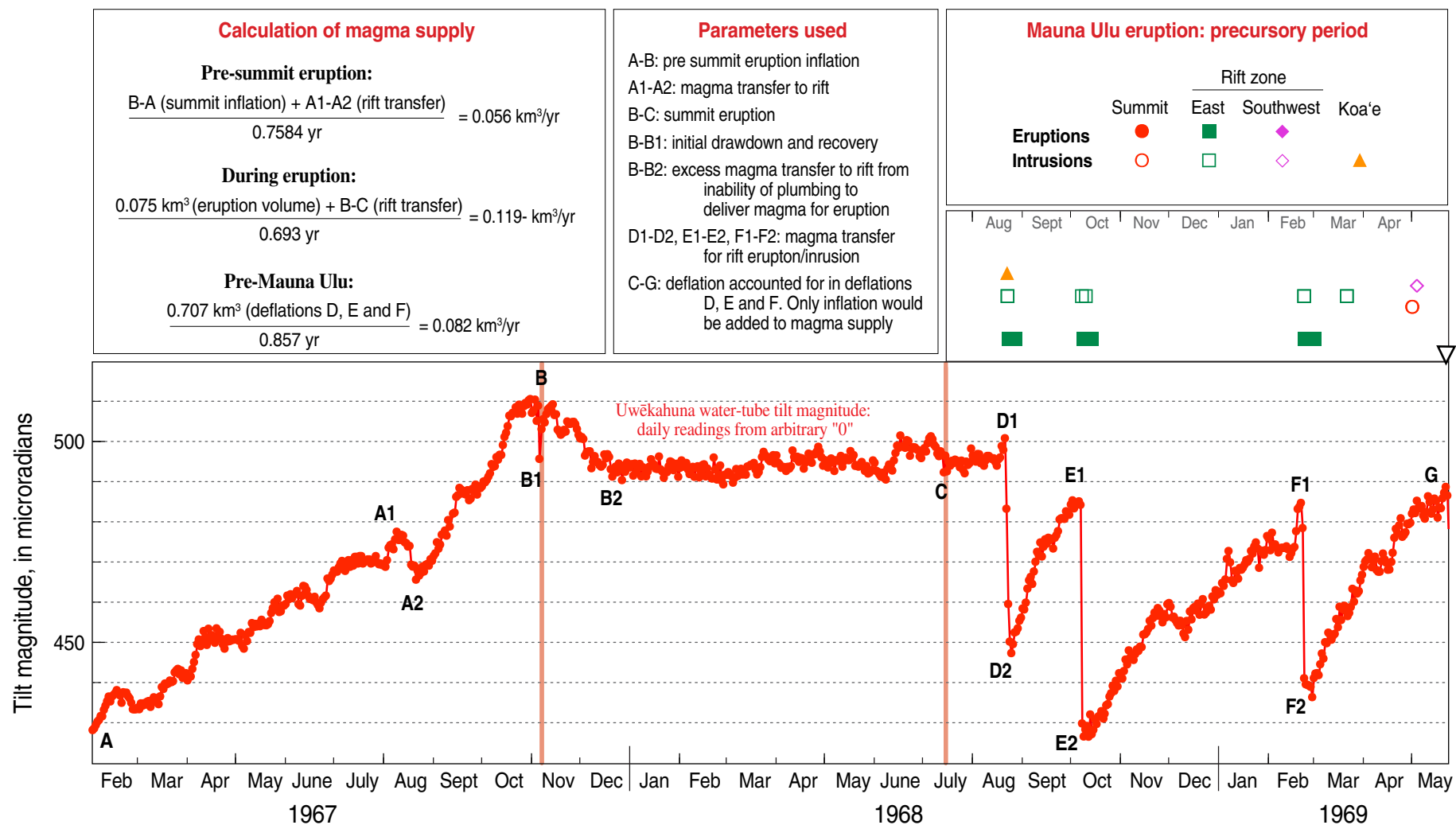


**Figure A5.** Calculation of magma supply—an example. Graphical depiction of the assumptions that go into our magma-supply calculations. See text for further explanation.



indicates shallow intrusion between the summit reservoir and the ground surface. For both cases the only quantity included in the calculations of magma supply rate is the net change over the entire eruptive period. To summarize, we calculate magma supply as follows (fig. A5):

Magma supply rate =  $\Sigma V_1 + V_2 + V_3$  (km<sup>3</sup>) /  $\Delta$  time (years).

$V_1$  = Lava volume of continuous eruption corrected to 80 percent of the published value to account for assumed 20 percent vesicles.

$V_2$  = Volume of summit inflation over the time period.

$V_3$  = Sum of all volumes of summit deflation over the time interval, used as a proxy for total volume of magma transfer to the rift zone(s).

Conversion of tilt to volume is calculated using the factor of 0.00045 km<sup>3</sup>/microradian (Dvorak and Dzurisin, 1993).

$\Delta$  time (years) = (ending date–beginning date)/365.25.

## Eruption Efficiency

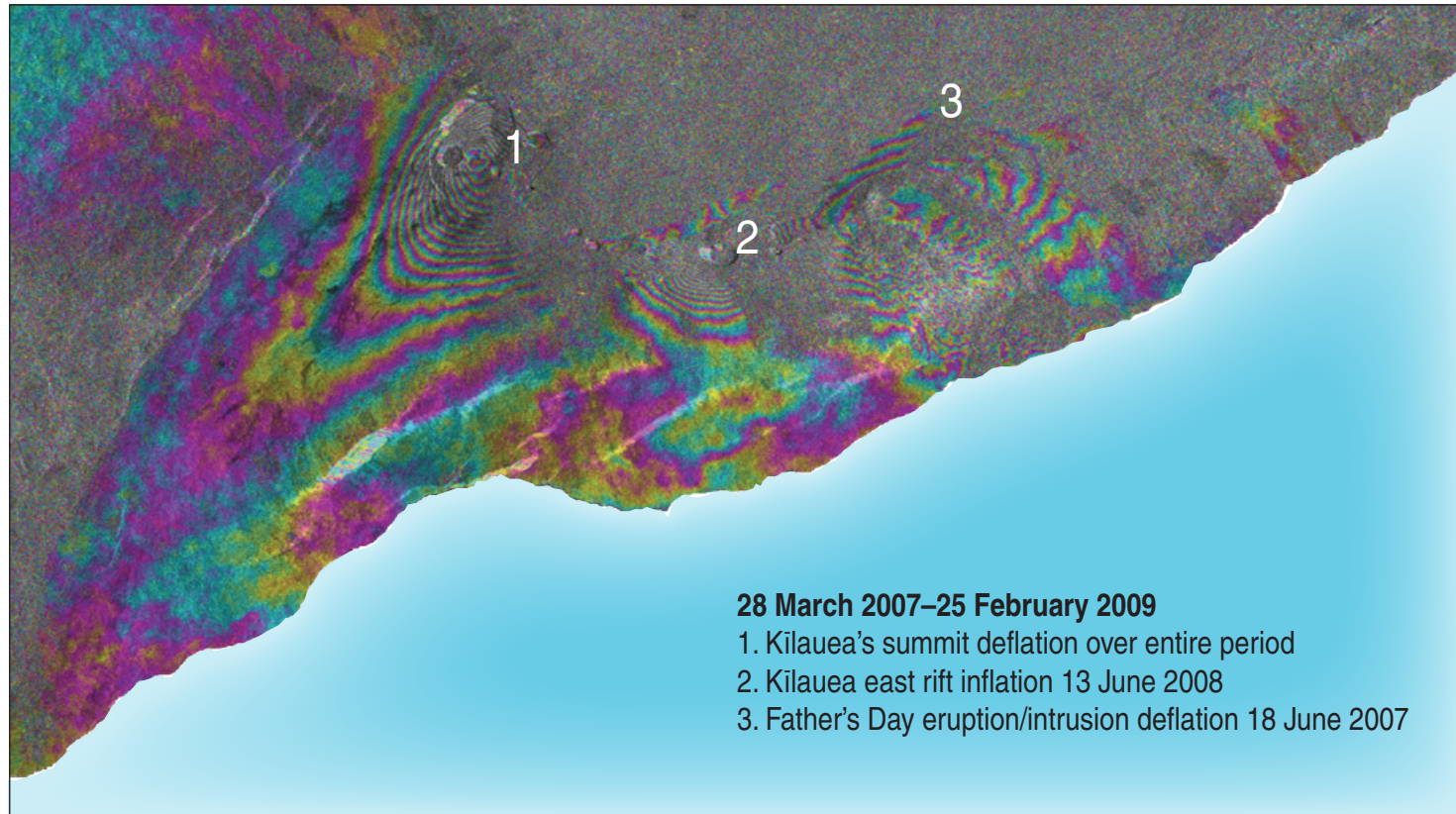
Rift eruptions are accompanied by a rapid deflation. In most cases the volume calculated from the deflationary tilt magnitude exceeds the volume of rift eruption and is used in the magma supply calculations as the amount of magma transferred to the rift zone. The ratio of erupted volume to tilt volume is recorded as “eruption efficiency,” varying between 0 (no eruption, all magma left underground as intrusion) and 1 (eruption volume equals tilt volume with negligible magma left as intrusion). This is an alternative way of looking at partitioning of magma between summit and rift to that published previously (Dvorak and Dzurisin, 1993, figure 10), and the results help validate the tilt-to-volume factor for intruded magma. For cases where the eruption efficiency exceeds 1, the tilt volumes are used in the magma supply calculations<sup>3</sup>.

---

<sup>3</sup> We assume that the uncertainties of lava volume estimates are larger than the uncertainties associated with assuming that the deflation source lies at a constant distance and depth relative to the summit tiltmeter.

## Summary

Looking at the entire Kīlauea history we face the same dilemma that John Dvorak faced in arriving at a tilt-to-volume factor, namely how to account for a range of latitude, longitude, and depth for modeled centers of inflation and deflation (Dvorak and Dzurisin, 1993). We find that changing the depth and (or) location within the limits of  $\pm 0.5$  km shown by the modeling does not compromise any of the conclusions reached regarding the variation of eruption efficiency with time. Thus we come to the same conclusion reached by Dvorak, namely that assumption of a constant for converting tilt magnitude to volume is appropriate, and therefore we use the Dvorak value.



Interferometric synthetic aperture radar (InSAR) satellite survey of Kilauea covering the time period 28 March 2007 to 25 February 2009. The most prominent pattern seen is deformation associated with the 18 June 2007 Father's Day eruption. In the colored interference bands, red inside blue indicates deflation (increased distance from the satellite to the ground), red outside blue indicates inflation (decreased distance). Hawaiian Volcano Observatory image courtesy of Michael Poland.

Menlo Park Publishing Service Center, California  
Manuscript approved for publication July 17, 2014  
Edited by Peter H. Stauffer  
Layout and design by Jeanne S. DiLeo

BACK COVER:

View of Kilauea's summit lava lake from the rim of Halema'uma'u Crater at dusk. The lava lake is in the informally named "Overlook" crater (from its location immediately below the former Halema'uma'u visitor overlook), set within the larger Halema'uma'u Crater. The lava surface is about 50 m (160 ft) below the rim of Overlook crater. At the right (southeast) margin of the lake, a persistent spattering source ejects spatter more than halfway up the crater wall. (USGS photograph by Matthew Patrick, taken 1 February 2014.)





